Appl Phys B (2009) 95: 475–482
DOI 10.1007/s00340-009-3461-8

Applied Physics B
Lasers and Optics

Vanadium-doped photorefractive titanosillenite crystal

R. Montenegro · A. Shumelyuk · R. Kumamoto · J.F. Carvalho · R.C. Santana · J. Frejlich

Received: 27 November 2008 / Revised version: 14 January 2009 / Published online: 19 March 2009

Abstract Holographic recording in a vanadium-doped $Bi_{12}TiO_{20}$ (BTO) photorefractive crystal puts into evidence a large hole–electron competition showing a fast and a slow hologram components. From the fast component evolution, some material parameters for the electron-donor photoactive centers are computed. The wavelength-resolved photoconductivity is shown to be strongly modified by V-doping compared to undoped and doped BTO with other elements. The increase of photoconductivity by green light preexposure is almost negligible here if compared with undoped BTO. Activation energy for dark conductivity measured for BTO:V is similar to that for undoped BTO, as measured close to room temperature, but sensibly lower than the value reported in the literature for a much higher temperature range. Optical absorption and EPR spectra do confirm already published results and suggestions about the possible role of vanadium in the sillenite structure.

PACS 42.65.Hw · 42.70.Nq · 42.65.-k · 72.20.Jv

1 Introduction

Photorefractive sillenite crystals are interesting materials for holographic recording and image processing applications. As most photorefractive materials, they exhibit a rich structure of defects the nature of which is still a matter of active research. They also exhibit a rather high optical activity and a rather low electro-optic coefficient. Doping of sillenites with different elements has been tried since long time ago in the hope to improve their characteristics (increase their electro-optic coefficient, enlarge the useful optical spectral range, reduce optical activity) and also to help better understanding the mechanisms and active centers involved in the recording process. Chmyrev et al. [1] have studied the effect of different dopants in $Bi_{12}MO_{20}$ (M = Si, Ge, Ti) and, as far as V is concerned, concluded that it enhances photosensitivity for $Bi_{12}TiO_{20}$ (BTO). Other researchers [2–4] have also focused on the effect of vanadium and of Ce, Pb [5], and Ru [6] in BTO. The inhibiting effect of Ga in sillenites [7, 8] has been also reported before. The optical and electrical characterization of doped (with Pb, Zr, Ga, V) and undoped sillenites, mostly BTO, was also reported [8–10], where deep and shallow centers were detected and partially characterized from a phenomenological point of view using optical, electrical, and combined techniques. Most of these papers, however, showed that doping always reduces the photoconductivity without sensibly improving other interesting properties.

Some degree of hole–electron competition has already been reported even for undoped sillenites, at least for BTO [9, 11, 12]. Such competition seems to be enhanced by doping, at least with Pb [9] and with V [2, 3]. In this paper we are focusing on V-doped BTO and show that in this case hole–electron competition is strongly enhanced giving rise to a fast and a slow hologram, where the latter prodominates in steady state, at least for 514.5-nm wavelength recording. We characterize these hologram components and some material parameters referred to the electron-donor photoactive

R. Montenegro · R. Kumamoto · J. Frejlich (✉)
Laboratorio de Óptica, IFGW-UNICAMP, Campinas, SP, Brazil
e-mail: frejlich@ifi.unicamp.br
Fax: +55-19-35212450

A. Shumelyuk
Institute of Physics, National Academy of Sciences, Kiev, Ukraine

J.F. Carvalho · R.C. Santana
Instituto de Física, UFG, Goiânia, GO, Brazil

centers. We show that the strong increase in photoconductivity exhibited by many sillenites by the action of preexposure under green light is negligeable in BTO:V. We also confirm a previous paper [4] indicating a strong decrease of $Bi^{3+} + h^+$ centers in V-doped BTO.

2 Experiments

The crystal under analysis is a V-doped BTO crystal (5.2 mm along axis [001], 4.7 mm along axis [$\bar{1}$10], and 2.4 mm along axis [110] that is considered as the thickness of the sample) that is labeled BTOV-J16a and was grown in the Federal University of Goiás at Goiânia, Brazil. Its composition, as measured by electron microanalysis using Wavelength Disperse Spectroscopy (WDS), is [4] $Bi_{12.04\pm0.08}Ti_{0.76\pm0.07}V_{0.16\pm0.02}O_{19.98}$. Several different experiments were carried out on this sample in order to characterize it.

2.1 Two-wave mixing recording and erasure

The crystal was placed in a holographic setup with the [001] axis perpendicular to the incidence plane (containing the incident recording beams and the input crystal plane normal directions) and perpendicular to the holographic vector $\vec{K}$, and the [$\bar{1}$10] axis parallel to $\vec{K}$. Holographic recording was carried out with intensities $I_R = 11.6$ mW/cm^2 and $I_S = 0.89$ mW/cm^2 at 514.5 nm with the angle between the incident beams being $2\theta = \pi/4$ and the input light polarization such as to ensure transmitted and diffracted beams with parallel polarizations at the crystal output for maximum beam coupling.

2.1.1 Self-stabilized holographic recording

Self-stabilized recording was carried out in the usual way on this sample, using the first harmonic component with amplitude [13]

$$I^{\Omega} \approx 4J_1(\psi_d)\sqrt{\eta}\sqrt{I_S^0\, I_R^0}\sin\varphi \tag{1}$$

as error signal in the feedback loop, which led to $\varphi = 0$, where the latter is the phase shift between parallel transmitted and diffracted beams behind the crystal. The second harmonic

$$I^{2\Omega} \approx 4J_2(\psi_d)\sqrt{\eta}\sqrt{I_S^0\, I_R^0}\cos\varphi \tag{2}$$

with $I^{2\Omega} \propto \sqrt{\eta}$ for $\varphi = 0$ was used to follow the evolution of the recording. Under externally applied field (few kV/cm), one of the selected phases ($\varphi = 0$ or π) in the feedback produced a running hologram, whereas for the opposite π-shifted phase, the recorded hologram was almost stationary. Hologram erasure experiments showed that in the former case only a fast (electron-based) hologram had been recorded, whereas in the latter case a strong hole–electron competition results giving rise to fast and slow hologram components with the latter predominating in steady state. The recording of an electron-based self-stabilized running hologram is certainly enabled by the higher speed of electrons, whereas an almost stationary self-stabilized hologram is possible because of the larger value (under steady state condition) of the hole–electron competition arising slow hologram component.

2.1.2 Hologram erasure

Holographic erasure experiments were carried out by switching off the weaker beam and illuminating the crystal with the stronger one and measuring the evolution of the diffracted light. In this particular case recording was not stabilized and was carried out without externally applied field. The evolution of a hologram produced by charge carriers of opposite signs that are excited from different photoactive centers in the band gap can be described by a set of two coupled differential equations as reported by references [12, 14–16] among many others. It is possible to show that in these conditions fast ("f") and slow ("s") holograms arise as described by the equation

$$\eta(t) = c + \left| A_f\, e^{-t/\tau_f} - A_s\, e^{-t/\tau_s} \right|^2 \tag{3}$$

with

$$\tau_f \approx \tau_{\mathrm{sc}}^e \tag{4}$$

$$\tau_s \approx \frac{\tau_{\mathrm{sc}}^h}{1 - \kappa_{12}\kappa_{21}} \tag{5}$$

and

$$\tau_{\mathrm{sc}}^e = \tau_M^e \left[\frac{1 + K^2 L_D^2}{1 + K^2 l_s^2}\right]_e \approx \frac{\epsilon\varepsilon_0\alpha d}{\sigma_e(0)(1 - e^{-\alpha d})}\left[1 + K^2 L_D^2\right]_e \tag{6}$$

$$\tau_{\mathrm{sc}}^h = \tau_M^h \left[\frac{1 + K^2 L_D^2}{1 + K^2 l_s^2}\right]_h \approx \tau_M^h = \frac{\epsilon\varepsilon_0\alpha d}{\sigma_h(0)(1 - e^{-\alpha d})} \tag{7}$$

where the approximations in (4) and (5) derive from the assumption $\tau_s \gg \tau_f$. Here we follow the notation in [12] with the indexes "e" being for "electrons" and "h" for "holes," where $\tau_M^{h,e}$ is the Maxwell relaxation time, and $\sigma_{h,e}(0)$ is the photoconductivity at the input plane inside the crystal. The dielectric constant is $\epsilon = 47$, $\varepsilon_0 = 8.85 \times 10^{-12}$ sm$^{-1}\,\Omega^{-1}$, the optical absorption coefficient at 514.5 nm is $\alpha = 412$ m^{-1} with the thickness $d = 2.4$ mm. From prior experiments we substituted $K^2 L_D^2 \approx 1.7$ for electrons and assumed that $K^2 L_D^2 \ll 1$ for holes (L_D: diffusion length) and $K^2 l_s^2 \ll 1$ for both with l_s being the Debye

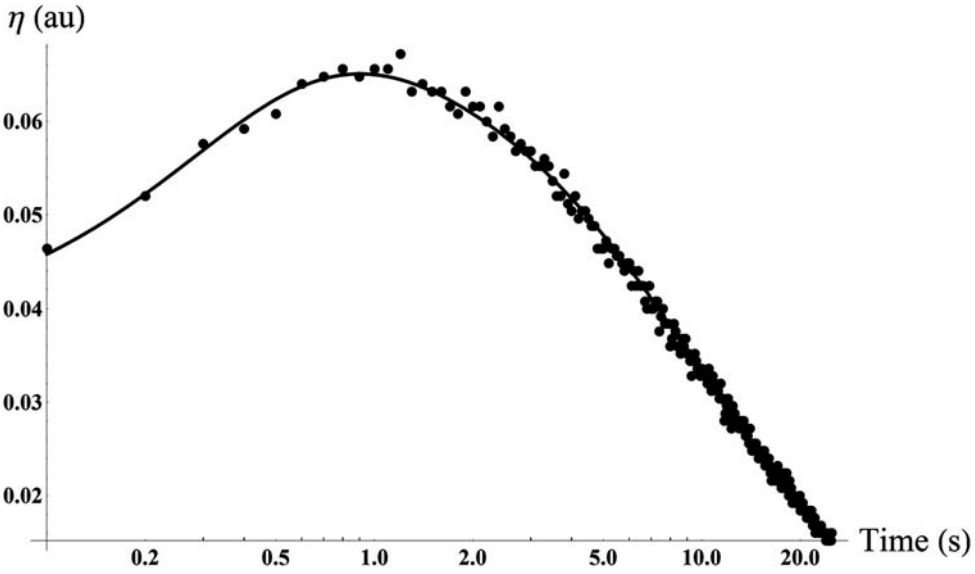

Fig. 1 Diffraction efficiency (au) as a function of time (seconds, in logarithmic scale) data (•) during the erasure of a hologram recorded on BTO:V with 514.5-nm wavelength without externally applied field and without stabilization at 514.5 nm. The *continuous line* is the theo-retical fitting

Table 1 Photoconductivity coefficient and sensitivity at 514.5 nm

		BTOV		BTO	BTO-005*	BTO:Pb
		Fast	Slow			
$\mathcal{S}$ (10^{-10} m^3/J)		32	0.65	53	52	60
$\sigma(0)h\nu/I_R(0)$ (10^{-30} sm/Ω)	Hologr.	27	–	60	95	60
	WRP	9		180	–	80

*Produced in the former USSR

screening length. The coupling constants are defined [12] as

$$1/\kappa_{12} \equiv 1 + K^2 l_{se}^2 - \imath K l_{Ee} \tag{8}$$

$$1/\kappa_{21} \equiv 1 + K^2 l_{sh}^2 - \imath K l_{Eh} \tag{9}$$

Equations (4–7) show that the fast hologram time constant is just that one characterizing the electron-based hologram buildup, whereas the slow one is related to that of the hole-based hologram, where the electrical couplings (κ_{12} and κ_{21}) between electrons and holes are also included. Diffraction efficiency erasure data (•) evolution in Fig. 1 actually shows a typical hole–electron competition erasure curve with holes and electrons on different localized states in the band gap of BTO:V. The first (overall growing efficiency up to about 1 s) part in the figure shows the erasure of the faster grating, whereas the second (decreasing) part is the erasure of the slower grating. From data fitting with (3), as shown by the continuous curve, the following parameters were obtained:

$$A_f = 0.17, \qquad A_s = 0.25 \tag{10}$$

$$\tau_f = 0.28 \text{ s}, \qquad \tau_s = 20 \text{ s} \tag{11}$$

with $c = 0.011$ being the background.

From (4) and (6) it is possible to compute the photoconductivity coefficient (photoconductivity per incident photon, in "second meter/Ohm" units) for electrons

$$\sigma_e(0)h\nu/I_R(0) = q\mu_e\tau_e\Phi_e\alpha \approx 27 \times 10^{-30} \text{ sm}/\Omega \tag{12}$$

where "(0)" means "at the input plane inside the crystal," $h\nu$ is the photonic energy, μ_e and τ_e are the electron mobility and lifetime in the conduction band, Φ_e is the quantum efficiency of photoelectron generation, and $I_R(0) = I_R^0(1-R)$ with I_R^0 and $I_R(0)$ being the irradiance of the erasing beam at the input crystal plane outside and inside the sample, respectively, with the reflectance $R \approx 0.2$. The photoconductivity coefficients above are reported in Table 1 together with the values measured for other doped and undoped BTO in the same setup. Data measured from wavelength-resolved photoconductivity (WRP) experiments [8] at the same 514.5-nm wavelength are also reported for comparison. Note that values from holographic techniques are systematically lower than those from WRP. We believe that this difference is due to the fact that absorption coefficients are computed in different ways for both experiments: for holography, the absorption was measured in a usual spectrophotometer, whereas for WRP, the absorption was measured with a photodetector very close to the sample, in which case

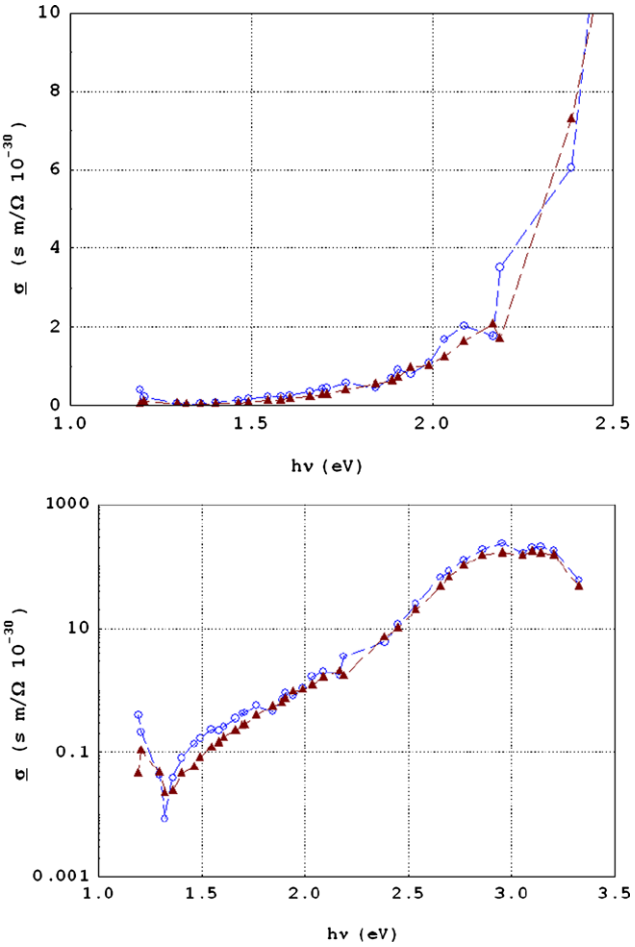

Fig. 2 Photoconductivity coefficient $\sigma h\nu/I_R(0)$ (sm/Ω) for BTO:V in relaxed (*circles*) and preexposed to 2.4-eV light (*triangles*) conditions on different scales to appreciate details: *top* figure in linear scale and *bottom* figure in logarithmic scale

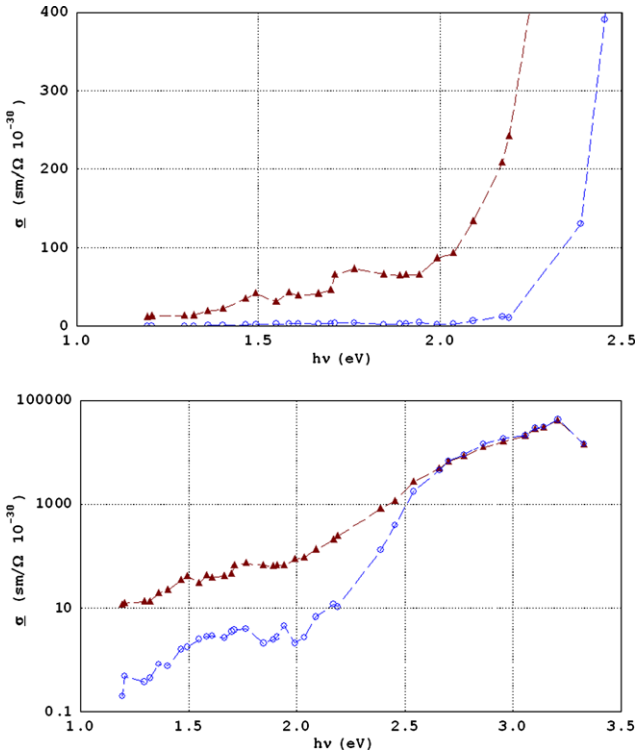

Fig. 3 Photoconductivity coefficient $\sigma h\nu/I_R(0)$ (sm/Ω) for undoped BTO in relaxed (*circles*) and pre-exposed to 2.4 eV light (*triangles*) conditions on different scales to appreciate details: *top* figure in linear scale and *bottom* figure in logarithmic scale

luminescence effects usually result in a lower apparent absorption coefficient [17]. Photoconductivity (and sensitivity) shown in Table 1 for fast and slow holograms in BTO:V cannot be directly compared with data for other crystals in this table because the latter are mainly for electrons.

2.1.3 Sensitivity

From (10) and (11) we compute the holographic sensitivity [13] associated to the fast and slow components that are respectively

$$\mathcal{S}_{f,s} = \frac{\lambda}{\pi m I_{\text{abs}}} \left[\frac{\partial \sqrt{\eta_{f,s}}}{\partial t} \right]_0 \tag{13}$$

where

$$\left[\frac{\partial \sqrt{\eta_{f,s}}}{\partial t} \right]_0 = A_{f,s}/\tau_{f,s} \tag{14}$$

$$I_R^{\text{abs}} = I_R^0 \frac{(1-R)(1-e^{-\alpha d})}{1 - R\, e^{-\alpha d}} \tag{15}$$

Here I_R^{abs} represents the absorbed erasing beam irradiance. From $m \approx 0.5$ we compute

$$\mathcal{S}_f = 32 \times 10^{-10}\ \text{m}^3/\text{J} \tag{16}$$

$$\mathcal{S}_s = 0.65 \times 10^{-10}\ \text{m}^3/\text{J} \tag{17}$$

$$\mathcal{S}_f/\mathcal{S}_s \approx 50 \tag{18}$$

As expected, the sensitivity is controlled by the faster hologram, and its value (together with that of the slower one) is reported in Table 1 and compared with those measured for other undoped and doped BTO in the same setup.

2.2 Wavelength-resolved photoconductivity

Wavelength-resolved photoconductivity (WRP) experiments were carried out as described elsewhere [17], and the result is shown in Fig. 2. Results for undoped BTO are shown in Fig. 3 for comparison. BTO:V shows the characteristic sharp step in WRP spectra at 2.2 eV but, differently from undoped BTO, exhibits a steadily increasing spectra without steps in the 1.2–2.2 eV range and shows almost no preexposition effects with 2.4-eV illumination.

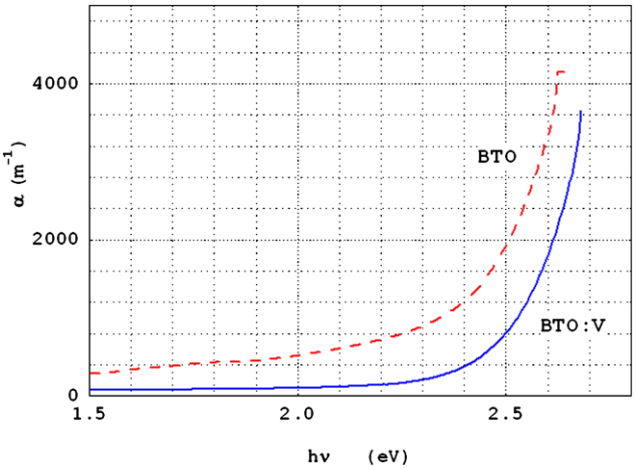

Fig. 4 Optical intensity absorption coefficient

2.3 Optical absorption

The optical intensity absorption coefficient of BTO:V is shown in Fig. 4, where we see that the absorption shoulder close to the band gap and starting by 2.4 eV is weaker than for undoped BTO. It is believed that this shoulder is mainly due to the $Bi^{3+} + h^{+}$ center occupying the Ti^{4+} vacancy in the characteristic sillenite oxygen tetrahedral [18] and its lower value may indicate a lower concentration of these centers. This result may indicate that at least part of the $Bi^{3+} + h^{+}$ centers (acting simultaneously as acceptors and donors) are here substituted by alternating V^{3+} and V^{5+} centers, thus dramatically reducing the overall photoconductivity compared to that for other crystals as reported in Table 1.

2.4 Dark conductivity

Dark conductivity in photorefractive materials can be measured using different techniques including direct electric (dc using an electrometer, ac using the so-called impedantiometric technique, or just a simple lock-in amplifier) and holographic techniques. The large hole–electron competition in BTO:V makes it difficult to use holographic techniques, so that we restricted ourselves to direct electric (dc or ac) techniques.

2.4.1 Direct electric techniques

The current in the dark was measured in our laboratory as a function of the applied voltage for different frequencies as illustrated in Fig. 5. From these data the complex ac conductance

$$C(\omega) \equiv \left[C_{\mathrm{dc}} + A\omega^{s}\right] + \imath B\omega \tag{19}$$

was measured as a function of the (angular) frequency ω for different temperatures as illustrated in Fig. 6. Note that,

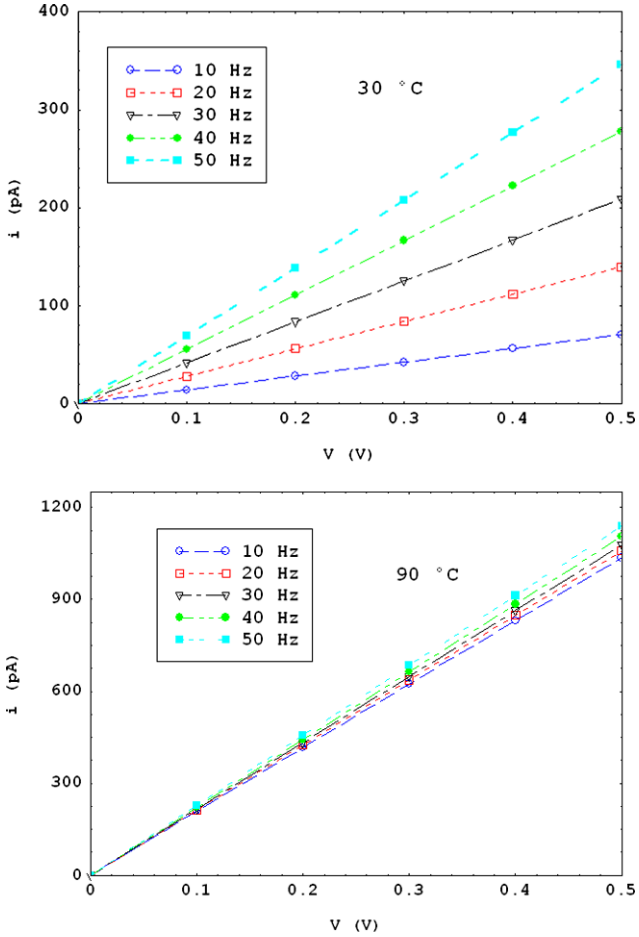

Fig. 5 Absolute value of the complex dark current (pA) as a function of the applied voltage for different frequencies varying from 10 to 50 Hz, for BTO:V at 30°C (*top*) and 90°C (*bottom*)

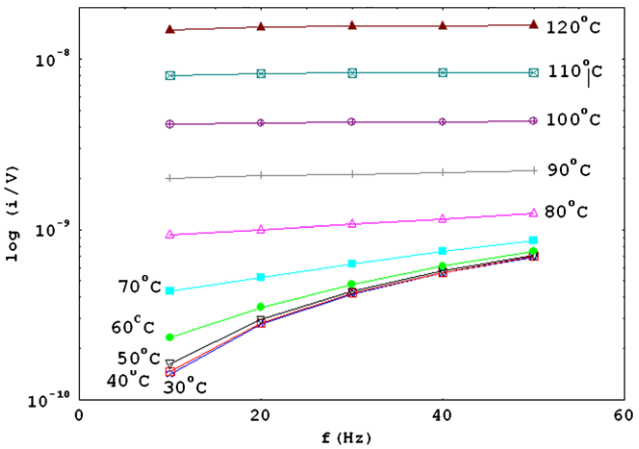

Fig. 6 Frequency dependence of the absolute value of the dark conductance $|C(\omega)|$ (A/V units) in log-scale for different temperatures from 30 to 120°C as measured on BTO:V

as the temperature increases, the frequency dependence is less pronounced as clearly shown in Fig. 6. The conductance is then extrapolated to $\omega = 0$ by fitting experimental

data with (19). In this case data fitting required adjusting the s-exponential of ω in the real part of the complex conductance. The presence of a term in ω in the real part of the conductance is an indication of a hopping mechanism instead of a band transport mechanism involved in the process [19, 20]. The dc dark conductance C_{dc} thus obtained, for temperatures in the range 30–120° C, gave a typical Arrhenius curve, as seen in Fig. 7. From this curve the dark conductivity activation energy is computed to be 0.89 for BTO:V as reported in Table 2 together with that for undoped and other doped BTO for comparison. Note that these values are, except for Ga-doped BTO, lower than those close to 1 eV reported from impedantiometric techniques [6, 21] although at a much higher temperature. The dark conductivity of BTO:V as extrapolated to 30°C is 60-fold larger than that for undoped BTO measured in the same conditions.

Our lower activation energies may indicate that dark conductivity in the room temperature range could be controlled by hopping or by tunneling, whereas at higher temperature it could be rather controlled by excitation to extended (probably valence band) states.

2.5 EPR spectra

Papers by Baquedano et al. [22] and Carvalho et al. [4] reported an isotropic nearly Lorentzian EPR line for a BSO crystal at room temperature (RT) and at 90 K that appeared to be due to a hole center rather to an electron. This confirms the presence of a $Bi^{3+} + h^{+}$ defect in the M^{4+} (M = Ti, Si, Ge) vacancy in the center of the oxygen tetrahedral sillenite structure referred to by many researchers.

An isotropic EPR line centered at $g = 2.006$ was also observed by Carvalho et al. [4] on BTO at 20 K and a much weaker one for g in the interval 1.9981–1.9984 for BTO:V without evidences of an EPR line for V, thus indicating the latter to be in the nonparamagnetic valences +5 and/or +3 and showing that the $Bi^{3+} + h^{+}$ centers are most of them being substituted by V^{3+} and/or V^{5+} on the tetrahedric site. New EPR spectra were now measured in this work on a BTO:V and undoped BTO single crystals at room temperature in an ESP-300 Bruker spectrometer working at 9.8 GHz, with standard Bruker cavity operating with 100 kHz magnetic field modulation with a microwave power of 5 mW. The frequency was measured with a Hewlett Packard 5350B microwave counter. The new spectra in Fig. 8 confirmed the presence of a strong line probably arising from a hole (h^{+}) in the oxygen tetrahedral in BTO that is dramatically reduced in BTO:V.

3 Discussion

We have investigated the strong hole–electron competition due to donors and ionized donors on different localized

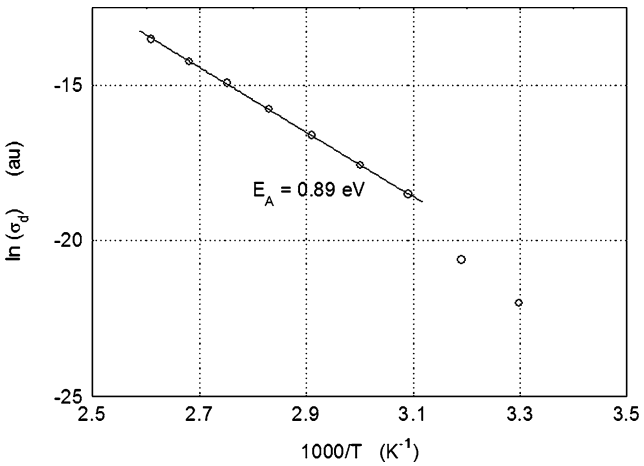

Fig. 7 Dark conductivity for BTO:V plotted as a function of inverse temperature with Arrhenius fitting (*solid line*) giving a 0.89 eV activation energy

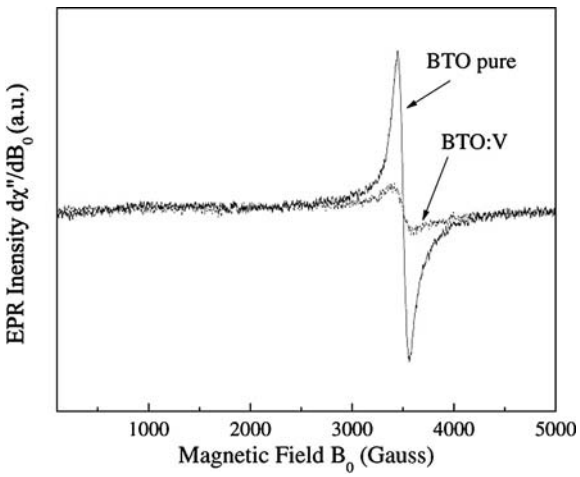

Fig. 8 EPR spectra of undoped and V-doped BTO showing a large symmetric signal indicating a hole in a symmetric environment (probably the oxygen tetrahedral site) for the former and a strong reduction of such a hole in the latter

Table 2 Dark conductivity activation energy (eV)

Sample	30–120°C	150–250°C	higher than 300°C
BTO	0.83	1.06 [6]	0.99 [21]
BTO:V	0.89	–	–
BTO:Pb	0.80	–	–
BTO:Ga	0.66	0.48 [24]	–

states in the band gap of BTO:V that produces a fast and a slow holographic component. Self-stabilized holographic recording techniques allow one to select whether to record an electron-based only hologram or a combined hole- and electron-based one by adequately selecting the operating conditions in the feedback stabilization loop.

The present work do confirm previous reports indicating that V-doping may reduce the density of $Bi^{3+} + h^{+}$ centers (that act as photoactive donors and acceptors) which might be at least partially substituted by V^{3+} and/or V^{5+} ions. The phenomenological effect of V-doping is a large increase in dark conductivity, a majoritary participation of deep photoactive acceptor centers in optical recording and a dramatic reduction of photoconductivity and of preexposure effects with green light. The two former effects (dark conductivity and photoactive acceptors increasing) may be related since conductivity in the dark in sillenites is usually associated with holes and hole-donors. Doping with Pb has a similar effect on preexposition but produces a much reduced effect on photoconductivity. Other elements like Zr also reduce the photoconductivity and preexposition but in a much reduced scale. Another peculiar and unique feature of V-doped BTO is the lack of sensible steps in the 1.2–2.2 eV range of the WRP spectrum that are supposed to indicate the position of empty donor centers in localized states between the bottom of the conduction band and the Fermi level at 2.2 eV below it. The negligible light preexposure effect may be directly related to the absence of these levels for the preexposure green light to pump electrons to. The way vanadium acts to produce these effects and to increase the role of deep acceptor traps in the recording process is, however, unclear.

From the point of view of the chemical composition and according to Valant and Suvorov [23], the sillenite structure as represented by

$$\mathrm{Bi}_{12}\left(\mathrm{Bi}^{3+}_{0.8}\square_{0.2}\right)\mathrm{O}_{19.2} \tag{20}$$

is formed by Bi–O-coordinated octahedra sharing corners to form regular tetrahedra, where their centers are 80% occupied by Bi^{3+} and 20% vacant (□), as represented inside the parenthesis in (20). The vacant tetrahedra have four oxygen ions occupying their four corners, but in the Bi^{3+}-occupied tetrahedra one of the oxygens is replaced by the lone electron pair from the central Bi^{3+} ion. The incorporation of Ti^{4+} ions in the sillenite structure occurs by partially filling the tetrahedral vacancies and substituting the Bi^{3+} in the tetrahedra according to the formula

$$\mathrm{Bi}_{12}\left(\mathrm{Bi}^{3+}_{0.8-4x}\mathrm{Ti}^{4+}_{5x}\square_{0.2-x}\right)\mathrm{O}_{19.2+4x}, \quad 0 < x < 0.2 \tag{21}$$

Besides Bi^{3+} donors, photoactive acceptors should be also included in order to allow for space charge spatial modulation, as required to enable optical recording. Acceptors like Bi^{5+} cannot be included because they are believed [23] to be unstable at the high temperature the crystal is grown. Instead Bi^{3+} plus a hole h^{+} in the form of the 4+ ion $[Bi^{3+} + h^{+}]$ that is simultaneously a donor ($Bi^{3+} + h^{+} \rightarrow Bi^{5+} + e^{-}$) and an acceptor (ionized donor) ($Bi^{3+} + h^{+} + e^{-} \rightarrow Bi^{3+}$) is certain to be present. The introduction of this 4+ charged ion in the structure may follow the same pattern as with Ti^{4+}: one $[Bi^{3+} + h^{+}]$ filling a vacant tetrahedra site and four other substituting four Bi^{3+} with four oxygen ions completing the missing oxygens in the corners of the substituted tetrahedra and balancing the charges according to the following formula:

$$\mathrm{Bi}_{12}\left(\mathrm{Bi}^{3+}_{0.8-4x-4z}\left[\mathrm{Bi}^{3+} + h^{+}\right]_{5z}\mathrm{Ti}^{4+}_{5x}\square_{0.2-x-z}\right)\mathrm{O}_{19.2+4x+4z}, \quad 0 < x + z < 0.2 \tag{22}$$

It is still possible to optically pump electrons from donors (Bi^{3+} and) to produce new photoactive acceptors Bi^{5+} at room temperature, thus also explaining (at least partially) light preexposition effects in sillenites.

Still, according to Valant and Suvorov, the addition of vanadium to the compound above occurs by substituting the Bi^{3+} ions by V^{5+} and incorporating an oxygen ion without modifying the tetrahedral vacancies following the formula

$$\mathrm{Bi}_{12}\left(\mathrm{Bi}^{3+}_{0.8-4x-y-4z}\left[\mathrm{Bi}^{3+} + h^{+}\right]_{5z}\mathrm{V}^{5+}_{y}\mathrm{Ti}^{4+}_{5x}\square_{0.2-x-z}\right) \times \mathrm{O}_{19.2+4x+y+4z}, \quad 0 < x + z < 0.2, \quad 0 < 4x + y + 4z < 0.8 \tag{23}$$

Note that by reducing the density of Bi^{3+} centers an indirect reduction in $[Bi^{3+} + h^{+}]$ also occurs. For the sample in this paper with $y = 0.16$, $5x = 0.76$, and $4x + y + 4z = 0.78$, the formula above reduces to

$$\mathrm{Bi}_{12}\left(\mathrm{Bi}^{3+}_{0.02}\left[\mathrm{Bi}^{3+} + h^{+}\right]_{0.015}\mathrm{V}^{5+}_{0.16}\mathrm{Ti}^{4+}_{0.76}\square_{0.045}\right)\mathrm{O}_{19.98} \tag{24}$$

where the density of Bi^{3+} and $[Bi^{3+} + h^{+}]$ centers is strongly reduced by the presence of V^{5+}. As the exchange of electrons is essentially operated via these two centers, their lower concentration may explain the dramatic reduction in photoconductivity here. The donor Bi^{3+} is more directly affected by the introduction of vanadium, so that its relative concentration may be lower, and this fact may explain the relative decrease of donor centers observed in holographic experiments on BTO:V as reported above.

It is also possible that the presence of the highly charged V^{5+} ion in BTO:V may inhibit, to some extent, the formation of Bi^{5+} by electron pumping by light, thus contributing to the reduced preexposure effect reported for BTO:V.

4 Conclusions

BTO doping with V leads to very peculiar features in the behavior of this (and probably other) sillenite. Its charac-

teristics are not sensibly improved by V-doping, but these experiments and results allow one to get a somewhat deeper insight and open new questions about the nature of the material and about the mechanisms involved in optical recording in sillenites. Some possibilities were discussed about the effect that V may produce on the chemical nature of BTO, but this matter is still lacking solid experimental support and requires further experimental work.

Acknowledgements We acknowledge the Conselho Nacional de Ciência e Technologia (CNPq), the Fundação de Amparo à Pesquisa do Estado de São Paulo (FAPESP), and the Coordenação de Aperfeiçoamento de Pessoal de Nível Superior (CAPES).

References

1. V.I. Chmyrev, V.M. Skorikov, E.V. Larina, Doping effect on the optical, electro-optic, and photoconductive properties of $Bi_{12}MO_{20}$ (M = Ge, Si, Ti). Inorg. Mater. **42**, 381–392 (2006)
2. S. Riehemann, D. Dirksen, G. von Bally, Non-exponential build–up and decay of holographic gratings in $Bi_{12}Ti_{0.76}V_{0.24}O_{20}$ crystals. Solid State Commun. **95**, 529–532 (1995)
3. S. Riehemann, F. Rickermann, V. Volkov, A. Egorysheva, G. von Bally, Optical and photorefractive characterization of BTO crystals doped with Cd, Ca, Ga and V. J. Nonlinear Opt. Phys. Mater. **6**, 235–249 (1997)
4. J.F. Carvalho, R.W.A. Franco, C.J. Magon, L.A.O. Nunes, A.C. Hernandes, Optical and magnetic characterization of pure and vanadium-doped $Bi_{12}TiO_{20}$ sillenite crystals. Opt. Mater. **13**, 333–338 (1999)
5. J.F. Carvalho, A.C. Hernandes, Growth and optical characterization of cerium and lead-doped $Bi_{12}TiO_{20}$ sillenite single crystals. Cryst. Res. Technol. **40**, 847–851 (2005)
6. V. Marinova, S. Lin, V. Sainov, M. Gospodinov, K. Hsu, Light-induced properties of Ru-doped $Bi_{12}TiO_{20}$ crystals. J. Opt. A, Pure Appl. Opt. **5**, S500–S506 (2003)
7. C. Coya, C. Zaldo, V. Volkov, A. Egorysheva, K. Polgár, A. Péter, Gallium-induced inhibition of the photorefractive properties of sillenite crystals. J. Opt. Soc. Am. B **13**, 908–915 (1996)
8. J. Frejlich, R. Montenegro, T.O. dos Santos, J.F. Carvalho, Characterization of photorefractive undoped and doped sillenite crystals using holographic and photoconductivity techniques. J. Opt. A, Pure Appl. Opt. **10**, 104005 (2008)
9. J. Frejlich, R. Montenegro, N.R. Inocente Jr., P.V. dos Santos, J.C. Launay, C. Longeaud, J.F. Carvalho, Phenomenological characterization of photoactive centers in $Bi_{12}TiO_{20}$ crystals. J. Appl. Phys. **101**, 043101 (2007)
10. L. Mosquera, I. de Oliveira, J. Frejlich, A.C. Hernandes, S. Lanfredi, J.F. Carvalho, Dark conductivity, photoconductivity and light-induced absorption in photorefractive sillenite crystals. J. Appl. Phys. **90**, 2635–2641 (2001)
11. P.V. dos Santos, J.F. Carvalho, J. Frejlich, Direct near infrared photorefractive recording and pre-exposure controlled hole-electron competition with enhanced recording in undoped $Bi_{12}TiO_{20}$. Appl. Phys. B **81**, 651–655 (2005)
12. I. de Oliveira, J. Frejlich, Detection of resonance space-charge wave peaks for holes and electrons in photorefractive crystals. J. Opt. Soc. Am. B **26**, 1298–1302 (2007)
13. J. Frejlich, *Photorefractive Materials: Fundamental Concepts, Holographic Recording, and Materials Characterization* (Wiley-Interscience, New York, 2006)
14. S. Zhivkova, M. Miteva, Holographic recording in photorefractive crystals with simultaneous electron-hole transport and two active centers. J. Appl. Phys. **68**, 3099–3103 (1990)
15. A. Shumelyuk, S. Odoulov, G. Brost, Nearly degenerate two-beam coupling. J. Opt. Soc. Am. B **15**, 2125–3131 (1998)
16. B. Sturman, P. Mathay, H.R. Jauslin, S. Odoulov, A. Shumelyuk, Modeling of the photorefractive nonlinear response in $Sn_2P_2S_6$ crystals. J. Opt. Soc. Am. B **24**, 1303–1309 (2007)
17. R. Montenegro, N.R. Inocente-Junior, J. Frejlich, New possibilities for the measurement of wavelength-resolved photoconductivity. Rev. Sci. Inst. **77**, 043905 (2006)
18. R. Oberschmid, Absorption centers of $Bi_{12}GeO_{20}$ and $Bi_{12}SiO_{20}$ crystals. Phys. Stat. Sol. A **89**, 263–270 (1985)
19. S.R. Elliot, A theory of a.c. conduction in chalcogenide glasses. Philos. Mag. **36**, 1291–1304 (1977)
20. V. Marinova, M. Hsieh, S. Lin, K. Hsu, Effect of ruthenium doping on the optical and photorefractive properties of $Bi_{12}TiO_{20}$ single crystals. Opt. Commun. **203**, 377–380 (2002)
21. S. Lanfredi, J.F. Carvalho, A.C. Hernandes, Electric and dielectric properties of $Bi_{12}TiO_{20}$ single crystals. J. Appl. Phys. **88**, 283–287 (2000)
22. J. Baquedano, F. López, J. Cabrera, EPR of nominally pure $Bi_{12}SiO_{20}$. Sol. Stat. Commun. **72**, 233–236 (1989)
23. M. Valant, D. Suvorov, A stoichiometric model for sillenites. Chem. Mater. **14**, 3471–3476 (2002)
24. A. Lobato, S. Lanfredi, J.F. Carvalho, A. Hernandes, Synthesis, crystal growth and characterization of γ-phase bismuth titanium oxide with gallium. Mater. Res. **3**, 92–96 (2000)